Structures and Electronic Properties of $Al_7X^{0,-}$ and $Al_{13}X_{1,2,12}^-$ Clusters with X=F, Cl, and Br

Jiao Sun, Wen-Cai Lu,* Li-Zhen Zhao, Wei Zhang, Ze-Sheng Li,* and Chia-Chung Sun

State Key Laboratory of Theoretical and Computational Chemistry, Institute of Theoretical Chemistry, Jilin University, Changchun 130021, People's Republic of China

Received: December 14, 2006; In Final Form: February 5, 2007

The structures, binding energies, and electronic properties for Al_7X, Al_7X^-, $Al_{13}X^-$, $Al_{13}X_2^-$, and $Al_{13}X_{12}^-$ (X = F, Cl, Br) were studied at the B3LYP/6-311+G(2d,p) level. Among the systems studied, Al_7 and Al_{13} clusters in Al_7X and $Al_{13}X^-$ reveal alkali-like and halogen-like superatom characters, respectively. Al_7 can bind with one halogen atom to form a salt-like compound as $Al_7^{+\delta}-X^{-\delta}$. Al_{13}^- can combine with one halogen atom to form a diatomic halogen anion $Al_{13}X^-$. However, when adding more halogens, the superatom structure would be destroyed, resulting in low-symmetry compounds with the center Al atom moving toward the cluster surface. The structures of $Al_{13}X_{1,2,12}^-$ (X = F, Cl, Br) are similar to those of X = I; however, their binding energies and electron structures are much different. In addition, the analyses of the calculated NBO charges show that Cl and Br have similar properties, but much different from F, when interacting with the Al clusters. The Al−Cl and Al−Br bonds have more covalent character in Al_7X and $Al_{13}X_{2,12}^-$, in contrast to the corresponding Al−F bond, which has prominent ionic character.

Introduction

A promising area of research on nanoscale materials is to search for clusters that could serve as the building blocks of new materials. Magic clusters will play important role due to their special stability. Among various magic clusters, Al_7[1,2] and Al_{13}[2−7] might provide opportunities for the synthesis of novel materials. In various Grignard-type reactions and in relevant processes of chemical vapor deposition of components for microelectronic devices, the aluminum halide has been studied.[8−11]

In the Jellium model,[12] special metal clusters can be viewed as superatoms. Al_7 with 21 valence electrons, which is likely to lose one electron to form Jellium's filled shell Al_7^+ ($1s^21p^61d^{10}2s^2$), can be considered as analogous to a super alkali atom. The mass spectra indicate that the Al_7^+ has a special stability due to its unusually large peak.[13] Castleman's experimental group and co-workers reported an unusually abundant cluster Al_7I^- in the mass spectra of aluminum halide clusters generated by reactions of aluminum clusters with iodine.[1,2] The neutral $Al_7^+I^-$ cluster, in which the positively charged Al_7^+ with a better Jellium structure, may be more stable.

Al_{13} has 39 valence electrons, short of only one electron to meet 40 electrons of a filled shell configuration $1s^21p^61d^{10}2s^2-1f^{14}2p^6$, which is similar to a halogen atom against Al_7. Bergeron et al. suggested that the cluster's atomic nuclei and their innermost electrons are seen as a spherical positively charged core surrounded by valence electrons in electronic shells similar to those of atoms.[2−4] The calculated value of the electron affinity of Al_{13} is nearly the same as a Br atom, thus it is called superhalogen. The $Al_{13}I^-$ can be considered as polyhalide-like BrI^- by covalent bond.[2,3] In contrast to $Al_{13}I^-$, the interaction between Al_{13} and alkaline atom M (M = Li−Cs) is by ionic bond.[14−18]

For $Al_{13}I_x^-$ (x = 1−12) clusters, experimental reactivity and theoretical calculation studies show accordant results that the clusters exhibit pronounced stability for even numbers of I atoms.[2,3,6,7] Theoretical calculated results and the highest occupied molecular orbital (HOMO) analyses reveal that the enhanced stability is associated with complementary pairs of I atoms occupying the on-top sites on the opposing Al atoms of the Al_{13}^- core in $Al_{13}I_x^-$ (x = 1−12).[3] The calculated results reported by Han and Jung show that Al_{13}^- core in $Al_{13}I_n^-$ ($n \geq 6$ at PBE level or $n \geq 7$ at the B3LYP level) is a cage-like structure other than a distorted icosahedron structure.[6] Recently, the N. O. Jones theoretic group and the A. W. Castleman, Jr. experimental group have jointly shown that $Al_{13}I_x^-$ and $Al_{14}I_x^-$ consist of compact Al_{13}^- and Al_{14}^{++} cores for $x \leq 8$, respectively; for $x > 8$, the cores assume a cage-like structure associated with the charging of the cores.[7] They also reported ground state $Al_{14}I_3^-$ that can be expressed as a closed shell Al_{14}^{++} core, as an alkaline earthlike superatom, surrounded by three I^- ligands.[3,7]

The above studies are mostly focused on aluminum cluster interactions with I. The theoretical study by J. Jung et al. on the neutral $Al_{13}X$ (X = F, Cl, Br, I) clusters shows that Al_{13} core of $Al_{13}X$ does not have icosahedral structure, instead it is a significantly distorted structure with C_s symmetry.[5] One may wonder if Al_{13} can keep the very stable I_h structure in cluster anions $Al_{13}X^-$, $Al_{13}X_2^-$, and $Al_{13}X_{12}^-$, and what differences of the binding energies and electron structures will be for X = F, Cl, and Br compared to X = I. Al_7X and Al_7X^- (X = F, Cl, Br) with different characters from $Al_{13}X$ and $Al_{13}X^-$ are also studied. In addition, we try to explain the experimental result that HBr and HCl etch the Al_n^- clusters less efficiently than HI.

Computational Methods

The theoretical computations were performed with the GAUSSIAN 03 software.[19] The geometries were fully optimized and vibrational frequencies were computed at the B3LYP[20]/6-

* Corresponding authors. E-mails: wencailu@jlu.edu.cn; zeshengli@jlu.edu.cn.

10.1021/jp068591o CCC: $37.00
Published on Web 04/21/2007

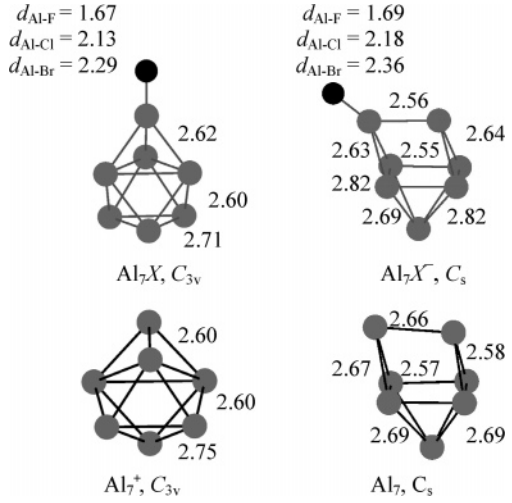

Figure 1. Comparison of optimized geometries of $Al_7^{0,+}$ and $Al_7X^{0,-}$ (X = F, Cl, Br) at the B3LYP/6-311+G(2df,p). Bond distances between halogen atom and its neighboring Al atom are in Å.

311+G(2df,p)//B3LYP/6-311G(d) for $Al_{13}X^-$, $Al_{13}X_2^-$, and $Al_{13}X_{12}^-$, and at the B3LYP/6-311+G(2df,p) for Al_7X and Al_7X^-. To find out the ground state, various possible initial structures and spin multiplicities were tried. Natural population analyses (NPA) and natural bond orbital (NBO) analyses were performed using the NBO 5.0[21] program as implemented in the GAUSSIAN 98 program. Nucleus-independent chemical shifts (NICS)[22] were calculated with using GIAO[23] at the B3LYP/6-311+G(2df,p) to evaluate the aromaticity.

In order to assess the computational approaches in studies of aluminum clusters, we also use the Kohn−Sham density functional theory (DFT) with a gradient-corrected exchange-correlation functional proposed by Perdew, Burke, and Ernzerhof (PBE),[24] implemented in the Dmol3 of the software package MATEPIALS STUDIO from Accelrys Inc.[25] The double numerical polarization (DNP) basis set and all-electrons was used, and were verified with vibrational frequencies calculations.

Results and Discussion

Al_7X and Al_7X^- (X = F, Cl, Br) Clusters. Figure 1 shows the ground-state geometries of $Al_7^{0,+}$ and $Al_7X^{0,-}$ with X = F, Cl, and Br, and the structural parameters are summarized in Table 1. We found that in the Al_7X relaxations, Al_7 changes to the Al_7^+ structure, and in the Al_7X^- relaxations, the Al_7 part keeps the similar structure as the Al_7 cluster. In Al_7X and Al_7X^-cases, the structures are very similar for X = F, Cl, and Br, which the Al−Al bond lengths are almost same for F, Cl, and Br, because of their same valence electronic structures. The only difference is the various bond lengths of Al−F, Al−Cl, and Al−Br. On the basis of the Jellium model, Al_7^+ can be considered as an alkali superatom, and Al_7X can act as a salt. As shown in Table 1, these large binding energies indicate that the Al_7−X bonds could be strong, and increase in the order I < Br < Cl < F. The NBO charge transfers from Al_7 to halogens are −0.77, −0.51, and −0.43 e^- for X = F, Cl, and Br, respectively. The Mulliken population analysis for Al_7X with X = Cl, Br, and I are similar. Therefore, we can consider that Al_7X is a jellium compound as $Al_7^{+\delta}-X^{-\delta}$ (X = F, Cl, Br, I), in which the positive charge of $Al_7^{+\delta}$ is mainly distributed on the link Al atom. The results are in good agreement with that of Al_7I.[1]

To examine the salt property of Al_7X, we have compared the binding energies of Al_7X with KX, which are 6.16, 4.51, and 3.95 eV for Al_7F, Al_7Cl, and Al_7Br, respectively, and 5.00, 4.21, and 3.86 eV for KF, KCl, and KBr, respectively. The larger halogen atomic radius corresponds to the smaller difference of binding energy between KX and Al_7X. The results of KX are in good agreement with experimental binding energies of 5.16, 4.49, and 3.93 eV responding to diatomic KF, KCl, and KBr at 298 K.[26]

Figure 2 shows orbital energy levels for Al_7, Al_7^+, and Al_7X. It is very interesting to note that the HOMO−LUMO gaps for Al_7X (X = F, Cl, Br, I) have the same value of 2.67 eV at the B3LYP functional and ∼1.8 eV at the PBE functional. The 2.67 eV is close to 2.75 eV for Al_7^+. The large stability of Al_7X can be expected by the relatively larger gap of Al_7^+ than its neighbored aluminum cluster cations. By comparing the orbital energy levels of Al_7, Al_7^+, and Al_7X, and analyzing the molecular orbital pictures and the orbital coefficients, we can find that the Al_7^+ fragment will contribute to the highest occupied orbitals as well as the lowest unoccupied orbitals of Al_7X, indicating that the HOMOs and LUMOs of Al_7X would be mainly located on the Al_7^+ fragment, other than the X^-. Therefore, the gaps for Al_7^+ and Al_7X with X = F, Cl, and Br are similar. The orbital analysis results are in agreement with Al_7I.[1] The X^- orbitals are found to locate at the lower energy levels: HOMO-3 with 2-fold, HOMO-6, and HOMO-8.

In Figure 3 the HOMOs and LUMOs for Al_7F and Al_7^+ are shown, which are completely similar. In order to analyze the Al_7F orbital property, we calculated the NICS values of Al_7F, and Al_7^+ and Al_6 substructures which are obtained by moving away the halogen atom and both the halogen and the top Al atom, respectively, as displayed in Figure 4. The points are chosen to range from 1.50 to 4.25 Å away from the link Al atom, and both B3LYP and HF calculations were performed. The results show that the NICS values, not sensitive to the methods, change continuously except for at 3.5 Å. The NICS curves of Al_7^+ and Al_7F are similar, in contrast to that of Al_6 which is positive and have a largest value (75.34 ppm) around the 3.5 Å point where a stronger antiaromaticity effect seems to occur. Thus the NICS kinks at about 3.5 Å for Al_7^+ and Al_7F may be related to the stronger antiaromaticity of the Al_6 part at this point. For Al_7X, the total NICS values at center are −79.43, −77.72, and −76.92 ppm with respect to X = F, Cl, and Br, which are close to the −74.17 ppm for Al_7^+. In our previous work, Al_7^+ has been shown to have aromatic character by a considerably large negative NICS value, the uniform bond lengths, and the large resonance energy (129.6 kcal/mol).[27] According to the above discussions, it can be expected that in Al_7X (X = F, Cl, and Br) the whole Al_7^+ part have similar valence orbitals and the aromatic character as Al_7^+.

Compared with Al_7X, negative Al_7X^- (X = F, Cl, Br, I) becomes the lower C_s symmetry, and Al−X bond length increases slightly. The charges on halogen atom and the link Al atom are less affected by the introduction of extra electron both at B3LYP and PBE functionals, which is consistent with the conclusion of ref[1] that the charge density of extra electron in Al_7I^- is mainly located around the Al_7 core. Therefore, in the Al_7X (X = F, Cl, Br, I) salt, the alkali-superatom Al_7^+ seems having a capability of containing extra electrons, based on the Jellium model with delocalized electrons. Such kind of materials containing magic aluminum clusters might be expected to be useful in future microelectronics.

$Al_{13}X^-$, $Al_{13}X_2^-$, and $Al_{13}X_{12}^-$ (X = F, Cl, Br) Clusters. The geometries of $Al_{13}X^-$, $Al_{13}X_2^-$, and $Al_{13}X_{12}^-$ (X = F, Cl, Br) clusters are shown in Figure 5, and the structure properties and energies are summarized in Table 2. In each case of $Al_{13}X^-$

TABLE 1: Bond Distances (Å), NBO Charges Q(*X*), HOMO−LUMO Gaps (eV), and Binding Energies (eV) for Al_7X and Al_7X^- (X = F, Cl, Br) Clusters[a]

cluster	d_{Al-X}	Q(*X*)	Q(link Al)	H−L gap	NICS(0)	E_b of *X*
Al_7F	1.67, 1.69[c]	−0.77, −0.49[b]	0.89, 0.48[b]	2.67, 1.80[b]	−79.43	6.16, 6.28[b]
Al_7Cl	2.13, 2.14[b]	−0.51, −0.36[b]	0.43, 0.33[b]	2.67, 1.80[b]	−77.72	4.51, 4.49[b]
Al_7Br	2.29, 2.30[b]	−0.43, −0.37[b]	0.31, 0.34[b]	2.67, 1.79[b]	−76.92	3.95, 3.90[b]
Al_7I	2.54[b]	−0.25,[c] −0.34[b]	0.19[c] 0.30[b]	1.74,[c] 1.78[b]		3.52,[c] 3.25[b]
	2.57[d]	−0.39[d]	0.34[d]	1.69[d]		2.94[d]
Al_7F^-	1.69, 1.72[b]	−0.79, −0.53[b]	0.82, 0.39[b]			6.05, 6.17[b]
Al_7Cl^-	2.18, 2.20[b]	−0.57, −0.46[b]	0.38, 0.26[b]			4.45, 4.44[b]
Al_7Br^-	2.36, 2.38[b]	−0.50, −0.49[b]	0.28, 0.28[b]			3.92, 3.87[b]
Al_7I^-	2.62,[c] 2.63[b]	−0.41,[c] −0.50[b]	0.15,[c] 0.25[b]			3.50,[c] 3.26[b]
	2.68[d]	−0.56[d]	0.29[d]			3.01[d]

[a] Geometries were optimized at the B3LYP/6-311+G(2df,p), binding energy with zero-point energy corrections is defined by $E_b(Al_7X^{0,-}) = E(X) + E(Al_7^{0,-}) - E(Al_7X)$. [b] At the PBE/DNP level using Dmol3. [c] Ref 1. [d] At the BLYP/DNP level using Dmol3.

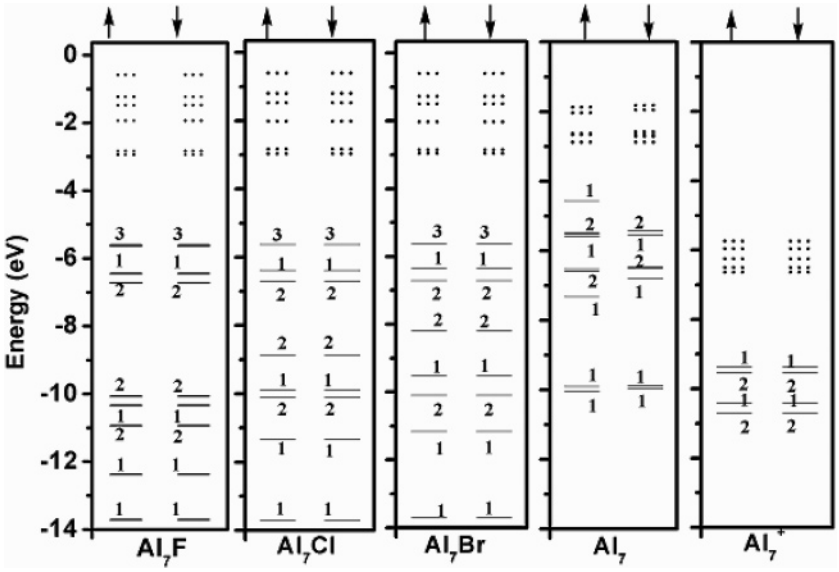

Figure 2. Orbital energy levels of the Al_7X (X = F, Cl, and Br), Al_7, and Al_7^+ clusters at the B3LYP/6-311G+(2df,p). Occupied orbital energy levels are indicated by solid lines, and unoccupied ones by dotted lines. Numbers 1, 2, or 3 indicate the degeneracy folds for occupied orbital energy levels.

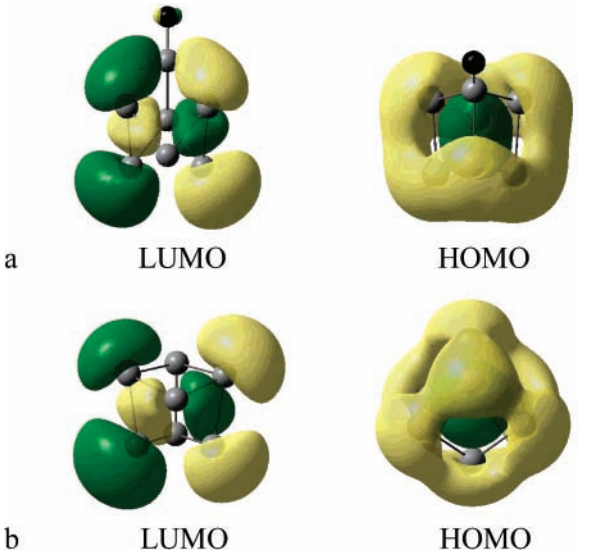

Figure 3. HOMOs and LUMOs (isodensity value is 0.02) for (a) Al_7F and (b) Al_7^+ at the B3LYP/6-311+G(2df,p).

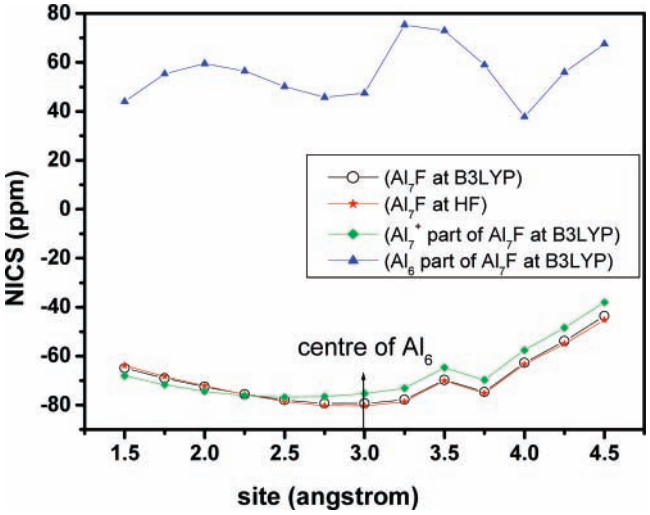

Figure 4. NICS values for Al_7F, and Al_7^+ and Al_6 parts in Al_7F at the B3LYP/6-311+G(2df,p).

and $Al_{13}X_2^-$, we started from initial configurations in which halogen atom is put at an on-top, bridge, or hollow site, respectively. In the optimized lowest-energy structures, the halogen likes to attach on the on-top site, and the Al_{13} core keeps I_h icosahedron in $Al_{13}X^-$(in the following, all symmetries we mention include the symmetries of the Al_{13} part), and C_s cage-like structures in $Al_{13}X_2^-$ and $Al_{13}X_{12}^-$. This is different from $Al_{13}I_x^-$ because in $Al_{13}I_x^-$ the Al_{13} cores assume a cage-like structure associated with the charging of the cores when $x > 6$[6] or $x > 8$.[7]

For $Al_{13}X^-$, halogen atom prefers to bind to a single Al atom and occupies an on-top site of I_h Al_{13}^- consistent with the case

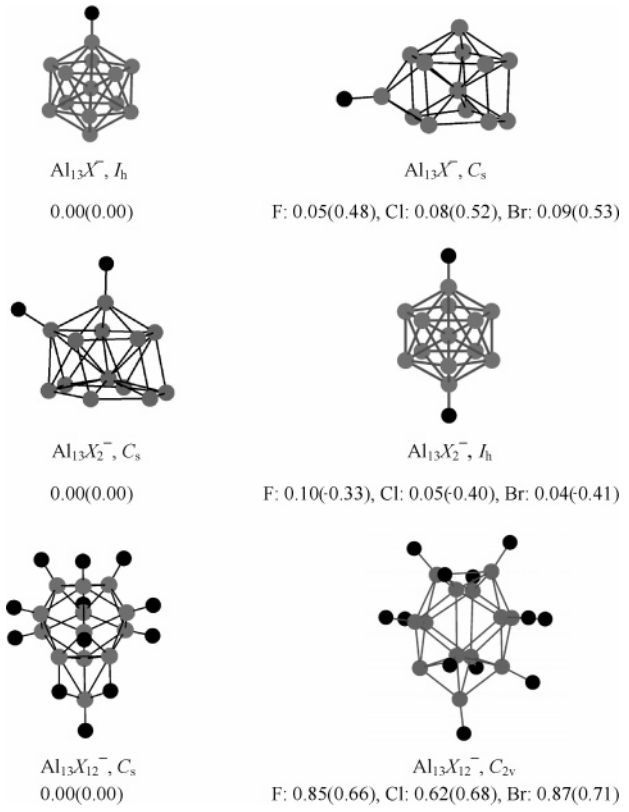

Figure 5. Optimized structures and relative energies (in eV) for $Al_{13}X^-$, $Al_{13}X_2^-$,and $Al_{13}X_{12}^-$ (X = F, Cl, Br) at the B3LYP/6-311G(d). The values in parentheses refer to the PBE/DNP relative energies.

of I atom attached to Al_{13}^-.[2-7] The binding energies of the isomers with the C_s cage-like structure are 0.046, 0.081, and 0.093 eV smaller than those of the I_h structures for $Al_{13}F^-$, $Al_{13}Cl^-$, and $Al_{13}Br^-$, respectively. The binding energies and HOMO−LUMO gaps of $Al_{13}X^-$ are smaller than those of $Al_{13}X_2^-$ and $Al_{13}X_{12}^-$ at both levels of the B3LYP/6-311G(d) and the PBE/DNP, showing the less stability of $Al_{13}X^-$ which is consistent with the experimental observations.[2,3] For $Al_{13}X^-$ with respect to X = F, Cl, and Br, the positive charges on the link Al atoms are +0.76, +0.27, and +0.14 e$^-$, the negative charges on halogen atoms are −0.78, −0.54, and −0.46 e$^-$, respectively, and the centered Al atom in the Al_{13} cage has the charge of about −1.5 e$^-$. The NBO charge analyses show a considerable difference of the charge distribution for X = F from X = Cl and Br, due to the remarkably large electronegativity of F.

For $Al_{13}X_2^-$, the C_s low-symmetry isomers turn to be the most stable structure and their energies are lower than those of the I_h isomers by 0.101 (F), 0.047 (Cl), and 0.041 (Br) eV, respectively. Here we would mention that the Dmol3 calculated results are opposite to the above results, i.e., I_h isomers are 0.326 (F), 0.401 (Cl), and 0.412 (Br) eV lower in energy than the corresponding C_s symmetry isomers. The differences of the energy order for the I_h and C_s isomers are resulted from the different functionals, B3LYP vs PBE, consistent with ref[6] which shows that for $Al_{13}I_2$, the I_h isomer is more stable at PBE, but less stable at B3LYP, compared with the C_s isomer. We also tested the single point energies of $Al_{13}X_2^-$ (X = F, Cl, and Br) at the MP2/6-311G(d) level, the energy order is consistent with that of PBE, i.e., the I_h isomer is more stable than the C_s isomer. The transformation from the I_h to the C_s or C_{2v} cage structures can be attributed to both electronic and steric reasons.[6] We think that electron delocalization is another factor causing the structural change from I_h to C_s or C_{2v}. Apparently, the electron delocalization in the HOMO of the C_s structure of $Al_{13}Br_2^-$ (Figure 6) would make the system more stable. In addition, the analyzing NBO charge indicates that $Al_{13}X_2^-$ can be regarded as an $Al_{13}^+2X^-$ structure. Thus, the C_s structure of $Al_{13}^+2X^-$ is expected to be favored due to the C_s symmetry of the most stable structure of Al_{13}^+. In contrast to $Al_{13}X_2^-$ (X = F, Cl, Br), the ground state of $Al_{13}I_2^-$ takes a I_h structure, which can be attributed to the weaker electronegativity and electron affinity of I.[6,7] The HOMO−LUMO gaps, 2.12 (F), 2.07 (Cl), and 2.07 (Br) eV, of the C_s isomers of $Al_{13}X_2^-$ are similar to each other and close to 2.18 eV of Al_{13}^+. For the I_h isomers of $Al_{13}X_2^-$, the HOMO−LUMO gaps are 2.40 (F), 2.42 (Cl), and 2.45 (Br), respectively, which are close to 2.53 eV for Al_{13}^-.

For $Al_{13}X_{12}^-$, the lowest-energy structures have C_s symmetry, which keep the I_h framework but the inner Al atom moves to the cluster surface, consistent with the previous reported results for $Al_{13}I_{12}^-$.[6,7] As is well-known, F, Cl, Br, and I are elements with large electronegativity, thus when the number of adsorbed halogen atoms increases, the system would be unstable if there is an inner Al atom carrying considerably negative charges. The inner Al tends to move toward the surface to provide electrons directly to halogen atoms. The isomers with C_{2v} symmetry are higher in energy than the C_s structures by 0.847, 0.625, 0.872 eV for X = F, Cl, and Br, respectively. At the PBE/DNP level in Dmol3, the obtained stable structures are consistent with those calculated by B3LYP using GAUSSIAN 03.

As shown in TABLE 2, the binding energies for Al_{13} halide anions decrease in the order: $Al_{13}X_{12}^- > Al_{13}X_2^- > Al_{13}X^-$ (X = F, Cl, and Br) (different from the order $Al_{13}I_2^- > Al_{13}I_{12}^-$), and correspondingly, the HOMO−LUMO gaps are getting smaller in this order. Note that the binding energies of $Al_{13}X_{1,2,12}^-$ are obviously smaller than those of Al_7X and Al_7X^-. In $Al_{13}X_{2,12}^-$, the charges on F atom are almost two times more than those on Cl or Br atoms; therefore, the Al−F bond of $Al_{13}F_{2,12}^-$ would have prominent ionic character relative to $Al_{13}X_{2,12}^-$ with X = Cl and Br.

On the basis of Al_{13}^-, the isoelectronic $Al_{12}Si$ species and $Al_{12}X$ (X = C, Ge, Sn, Pb)[28-32] with doped atom at center, have attracted considerable experimental and theoretical attention. The stable structures of $Al_{12}SiX$ (X = F, Cl, Br) are similar to the C_s isomers of $Al_{13}X^-$ with one Si atom replacing the centered Al atom. In $Al_{12}SiX$, the C_s structure is more favorable than the I_h structure for $Al_{12}Si^+$ part, which is different form $Al_{13}X^-$. For C_s and I_h $Al_{12}Si$, the adiabatic EAs with respect to the optimized structures of both neutral and cationic clusters, EA = $E(Al_{12}Si^+) - E(Al_{12}Si)$, are 6.505 and 6.655 eV, respectively, larger than those for F (3.457), Cl (3.684), and Br (3.553) eV at the same level of the B3LYP/6-311+G(2df,p). This suggest that in an isolated state, the $Al_{12}Si$ for both C_s and I_h symmetries is harder to lose an electron than halogen; however, it may transfer an electron to halogen atom easily due to the polarization and structural change induced by halogen. Since our calculated binding energies of $Al_{12}SiX$ are quite large with 4.856, 3.200, and 2.629 eV for X = F, Cl, Br, respectively, which are only slightly smaller than that for $Al_{13}X^-$.

The experiments show that in the interaction of aluminum with both MeX[8,10,33] and HX[4] (X = Cl, Br, and I), reactivity decreases upon ascension of the periodic table. There are probably two important factors to affect the reactivity with aluminum clusters. First, the polarizability of reactants decreases in the order I > Br > Cl. While at the beginning of alkyl halides or hydrogen halides adsorption on aluminum, van der Waals' potential may play an important role. Therefore, the stronger polarizability will lead to the easier complexation. Second, the

TABLE 2: Bond Distances (Å), NBO Charges Q(X), Q_{center}(Al) of the Al−X Bonds, HOMO−LUMO Gaps (eV), and Binding Energies (eV) for $Al_{13}X^-$, $Al_{13}X_2^-$, and $Al_{13}X_{12}^-$ (X = F, Cl, Br, I) Clusters[a]

cluster	d_{Al-X}	Q(*X*)	Q_{center}(Al)	H−L gap	E_b of *X*
$Al_{13}F^-$−I_h	1.71	−0.78	−1.47	1.63, 0.78[b]	5.05, 5.42[b]
$Al_{13}Cl^-$−I_h	2.18	−0.54	−1.45	1.63, 0.76[b]	3.48, 3.71[b]
$Al_{13}Br^-$−I_h	2.35	−0.46	−1.48	1.58, 0.74[b]	2.94, 3.15[b]
$Al_{13}F^-$−C_s	1.72	−0.77	−1.70	1.33, 0.47[b]	5.01, 4.94[b]
$Al_{13}Cl^-$−C_s	2.19	−0.54	−1.70	1.33, 0.47[b]	3.39, 3.19[bb]
$Al_{13}Br^-$−C_s	2.36	−0.47	−1.70	1.33, 0.47[b]	2.85, 2.62[b]
$Al_{13}F_2^-$−C_s	1.71	−0.77,[c] −0.78[d]	−1.32	2.12, 1.39[b]	5.52, 5.67[b]
$Al_{13}Cl_2^-$−C_s	2.18	−0.52,[c] −0.54[d]	−1.31	2.07, 1.34[b]	3.92, 3.94[b]
$Al_{13}Br_2^-$−C_s	2.35	−0.44,[c] −0.47[d]	−1.31	2.07, 1.33[b]	3.38, 3.36[b]
$Al_{13}F_2^-$−I_h	1.70	−0.77	−1.46	2.40, 1.73[b]	5.47, 5.83[b]
$Al_{13}Cl_2^-$−I_h	2.17	−0.52	−1.41	2.42, 1.75[b]	3.90, 4.14[b]
$Al_{13}Br_2^-$−I_h	2.33	−0.44	−1.41	2.45, 1.75[b]	3.36, 3.57[b]
$Al_{13}F_{12}^-$−C_s	1.70, 7.87	−0.72 to −0.75		2.20, 1.13[b]	5.58, 5.83[b]
$Al_{13}Cl_{12}^-$−C_s	2.30, 2.14	−0.37 to −0.46		2.53, 1.26[b]	3.96, 4.10[b]
$Al_{13}Br_{12}^-$−C_s	2.46, 2.30	−0.27 to −0.43		2.37, 1.23[b]	3.41, 3.52[b]
$Al_{13}F_{12}^-$−C_{2v}	1.69 ∼ 1.70	−0.74 to −0.76		2.04, 1.12[b]	5.51, 5.78[b]
$Al_{13}Cl_{12}^-$−C_{2v}	2.13 ∼ 2.15	−0.44 to −0.49		1.96, 0.99[b]	3.91, 4.04[b]
$Al_{13}Br_{12}^-$−C_{2v}	2.28 ∼ 2.31	−0.34 to −0.40		1.99, 0.94[b]	3.34, 3.46[b]
$Al_{13}I^-$−I_h	2.62,[b] 2.60[e]	−0.64,[b] −0.35[f]		0.71, [b]0.72[g]	2.48, [f]2.52[g]
$Al_{13}I_2^-$−I_h	2.58,[b] 2.58[f]	−0.48,[b] −0.35[f]		1.75, [b]1.74[g]	2.90, [f]2.94[g]
	2.62[h]	−0.56[h]		1.59[h]	2.72,[b] 2.44[h]
$Al_{13}I_2^-$−C_s	2.61[b]	−0.47[b]		1.29[b]	2.49[b]
	2.63[h], 2.65[h]	−0.54[h]		1.29[h]	2.45[h]
$Al_{13}I_{12}^-$−C_{2v}	2.53∼2.54[d]	−0.35[f]		0.84, [b]0.88[g]	2.85, [f]2.79[g]

[a] Geometries were optimized at the B3LYP/6-311G(d), and single-point energy calculations were performed at the B3LYP/6-311G+(2df,p); binding energy with zero point energy corrections is defined by $E_b(Al_{13}X_n^-) = [nE(X) + E(Al_{13}^-) - E(Al_{13}X_n^-)]/n$. [b] At the PBE/DNP level using Dmol3. [c] Halogen for top site. [d] Halogen for side site. [e] Ref 2. [f] Ref 7. [g] Ref 6. [h] At the BLYP/DNP level using Dmol3.

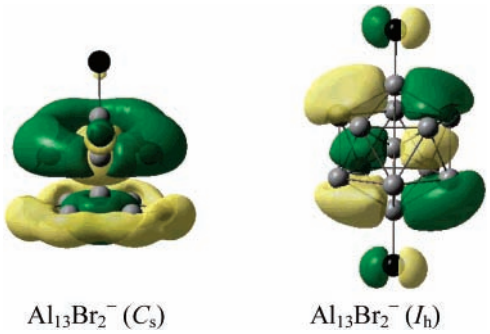

Figure 6. Comparison of HOMOs (isodensity value is 0.02) for C_s and I_h $Al_{13}Br_2^-$ calculated at the B3LYP/6-311+G(2df,p).

TABLE 3: Polarizabilities, Charges, and Wiberg Bond Order for H−X and Me−X (X = F, Cl, and Br) Molecules[a]

	HF	HCl	HBr	MeF	MeCl	MeBr
polar.	5.05	16.58	23.07	16.86	29.14	36.39
Q(X)	−0.55	−0.26	−0.19	−0.40	−0.07	−0.02
bond order	0.70	0.94	0.97	0.85	1.03	1.03

[a] Calculated at the B3LYP/6-311++G(3df,3p).

H−X and C−X bond strengths of the reactants increase in the order I < Br < Cl. According to the polarizability and stability of the reactants HX and MeX, the trend of reactivity should increase in the order Cl < Br < I.

In TABLE 3 we have shown the polarizabilities, charges of halogen atoms, and Wiberg bond indices (WBI) for MeX and HX (X = F, Cl, and Br) molecules. It can be seen from TABLE 3 that Cl and Br have similar character; however F is remarkably different from Cl and Br. In MeF and HF the F atom has abundant negative charges, considerably more than the charges on Cl and Br atoms, and the calculated values of WBI reveal that H−F and C−F bonds have prominent ionic character compared with the cases of Cl and Br. Therefore, MeF and HF with special ionic bond character can be easily adsorbed on the Al clusters, and meanwhile the Al clusters, with a larger tendency of losing electrons than C and H atoms, can transfer electrons to F atom easily. Thus MeF and HF would have strong etching action to Al clusters.

Conclusions

The $Al_7X^{0,-}$, $Al_{13}X_{1,2,12}^-$, and $Al_{12}SiX$ (X = F, Cl, Br) clusters were studied using DFT method. In Al_7X and $Al_{13}X^-$, the Al_7 and Al_{13} fragments with C_{3v} and I_h symmetries can be considered as alkali-like and halogen-like superatoms, and they are not only magic clusters but also possess character of electron delocalization. The HOMOs and LUMOs of the salt-like compound Al_7X and polyhalide-like $Al_{13}X^-$ are mainly located on the Al_7^+ or Al_{13} part. While Al_{13}^- binds with more halogen atoms, its I_h structure would transforms into C_s or C_{2v} low-symmetry structure.

For various halogen atoms including I, the most stable geometries are similar with each other except for $Al_{13}X_2^-$ (X = F, Cl, Br) with the C_s Al_{13} part different from that of I with the I_h Al_{13} part. However, the electronic structures and binding energies for different halogen atoms are much different. The calculated binding energies decrease in the order, F > Cl > Br, and from this trend the halides with *X* = I can be expected to have the smallest binding energy. When the number of halogen atoms gets larger, the binding energies for Al_{13} halide anions are shown to increase in the order: $Al_{13}X^- < Al_{13}X_2^- < Al_{13}X_{12}^-$ (X = F, Cl, and Br), different from the order for X = I, $Al_{13}I_2^- > Al_{13}I_{12}^-$. The calculated NBO charges show that Cl and Br are similar but are much different from F, when interacting with the Al clusters. The Al−F bond have obvious ionic character in contrast to the Al−X bonds (X = Cl and Br).

Acknowledgment. This work was supported by the National Natural Science Foundation of China (Nos. 20473030, 20333050, 60028403), Doctor Foundation of the Ministry of Education, and Foundation for University Key Teachers of the Ministry of Education of China, and Foundation of Innovation by Jilin University.

References and Notes

(1) Bergeron D. E.; Roach P. J.; Castleman, A. W., Jr.; Jones, N. O. Reveles, J. U.; Khanna, S. N.; *J. Am. Chem. Soc.* **2005**, *127*, 16048.

(2) Bergeron, D. E.; Castleman, A. W., Jr.; Morisato, T.; Khanna, S. N. *Science* **2004**, *304*, 84.

(3) Bergeron D. E.; Roach P. J.; Castleman, A. W., Jr.; Jones, N. O.; Khanna, S. N. *Science* **2005**, *307*, 231.

(4) Bergeron, D. E. A.; Castleman, W., Jr.; Morisato, T.; Khanna, S. N. *J. Chem. Phys.* **2004**, *121*, 10456.

(5) Jung, J.; Kim, J. C.; Han, Y.-K. *Phys. Rev. B* **2005**, *72*, 155439.

(6) Han, Y.-K.; Jung, J. *J. Chem. Phys.* **2005**, *123*, 101102.

(7) Jones, N. O.; Reveles, J. U.; Khanna, S. N.; Bergeron, D. E.; Roach, P. J.; Castleman, A. W., Jr. *J. Chem. Phys.* **2006**, *124*, 154311.

(8) Chen, J. G.; Beebe, T. P., Jr.; Crowell, J. E.; Yates, J. T., Jr. *J. Am. Chem. Soc*. **1987**, *109*, 1726.

(9) Mezhenny, S.; Sorescu, D. C.; Maksymovych, P.; Yates, J. T., Jr. *J. Am. Chem. Soc*. **2002**, *124*, 14202.

(10) Bent, B. E.; Nuzzo, R. G.; Zegarski, B. R.; Dubois, L. H. *J. Am. Chem. Soc*. **1991**, *113*, 1137.

(11) Lohokare, S.; Crane, E. L.; Dubois, L. H.; Nuzzo, R. G. *Langmuir* **1998**, *14*, 1328.

(12) Knight, W. D.; Clemenger, K.; Heer, W. A. de; Saunders, W. A.; Chou, M. Y.; Cohen, M. L. *Phys. Rev. Lett*. **1984**, *52*, 2141.

(13) (a) Hanley, L.; Ruatta, S.; Anderson, S. J. *Chem. Phys.* **1987**, *87*, 260. (b) Jarrold, M. F.; Bower, J. E.; Kraus, J. S. *J. Chem. Phys*. **1987**, *86*, 3876.

(14) Rao, B. K.; Khanna, S. N.; Jena, P.; *Phys. Rev. B* **2000**, *62*, 4666.

(15) Khanna, S. N.; Rao, B. K.; Jena, P. *Phys. Rev. B* **2002**, *65*, 125105.

(16) Majumder, C.; Das, G. P.; Kulshrestha, S. K.; Shah, V.; Kanhere, D. G.; *Chem. Phys. Lett.* **1996**, *261*, 515.

(17) Kumar, V. *Phys. Rev. B* **1998**, *57*, 8827.

(18) Ashman, C.; Khanna, S. N.; Pederson, M. R. *Phys. Rev. B* **2002**, *66*, 193408.

(19) Frisch, M. J.; Trucks, G. W.; Schlegel, H. B.; Scuseria, G. E.; Robb, M. A.; Cheeseman, J. R.; Zakrzewski, V. G.; Montgomery, J. A., Jr.; Stratmann, R. E.; Burant, J. C.; Dapprich, S.; Millam, J. M.; Daniels, A. D.; Kudin, K. N.; Strain, M. C.; Farkas, O.; Tomasi, J.; Barone, V.; Cossi, M.; Cammi, R.; Mennucci, B.; Pomelli, C.; Adamo, C.; Clifford, S.; Ochterski, J.; Petersson, G. A.; Ayala, P. Y.; Cui, Q.; Morokuma, K.; Malick, D. K.; Rabuck, A. D.; Raghavachari, K.; Foresman, J. B.; Cioslowski, J.; Ortiz, J. V.; Stefanov, B. B.; Liu, G.; Liashenko, A.; Piskorz, P.; Komaromi, I.; Gomperts, R.; Martin, R. L.; Fox, D. J.; Keith, T.; Al-Laham, M. A.; Peng, C. Y.; Nanayakkara, A.; Gonzalez, C.; Challacombe, M.; Gill, P. M. W.; Johnson, B. G.; Chen, W.; Wong, M. W.; Andres, J. L.; Head-Gordon, M.; Replogle, E. S.; Pople, J. A. *GAUSSIAN 03*, Revision B. 03; Gaussian, Inc.: Pittsburgh, PA, 2003.

(20) (a) Becke, A. D. *J. Chem. Phys*. **1993**, *98*, 5648. (b) Lee, C.; Yang, W.; Parr, R. G. *Phys. Rev. B* **1988**, *37*, 785. (c) Mielich, B.; Savin, A.; Stoll, H.; Preuss, H. *Chem. Phys. Lett*. **1989**, *157*, 200.

(21) Bohmann, J. A.; Weinhold, F.; Farrar, T. C. *J. Chem. Phys*. **1997**, *107*, 1173. *NBO3.0* is available in the *Gaussian 03* program, but the more advanced *NBO5.0* version be installed in *Gaussian 98*.

(22) Schleyer, P. v. R.; Maerker, C.; Dransfeld, A.; Jiao H.; Hommes, N. J. R. v. E. *J. Am. Chem. Soc.* **1996**, *118*, 6317.

(23) Wolinski, K.; Hilton, J. F.; Pulay, P. *J. Am. Chem. Soc.* **1990**, *112*, 8251.

(24) Perdew, J. P.; Burke, K.; Ernzerhof, M. *Phys. Rev. Lett*. **1996**, *77*, 3865.

(25) (a) Delley, B. *J. Chem. Phys*. **1990**, *92*, 508. (b) Delley, B. *J. Chem. Phys.* **1991**, *94*, 7245.

(26) *CRC Handbook of Chemistry and Physics*, 81st ed.: CRC Press: Boca Raton, FL, 2000.

(27) Sun, J.; Lu, W.-C.; Wang, H.; Li, Z.-S.; Sun, C.-C. *J. Phys. Chem. A* **2006**, *110*, 2729.

(28) Gong, X. G.; Kumar, V. *Phys. Rev. Lett.* **1993**, *70*, 2078.

(29) Seitsonen, A. P.; Puska, M. J.; Alatalo, M.; Nieminen, R. M.; Milman, V.; Payne, M. C. *Phys. Rev B* **1993**, *48*, 1981.

(30) Kumar, V.; Bhattacharjee, S.; Kawazoe, Y. *Phys. Rev. B* **2000**, *61*, 8541.

(31) Li, X.; Wang, L.-S. *Phys. Rev. B* **2002**, *65*, 153404.

(32) Charkin, O. P.; Charkin, D. O.; Klimenko, N. M.; Mebel, A. M. *Faraday Discuss.* **2003**, *124*, 215.

(33) Bergeron, D. E.; Castleman, A. W., Jr. *Chem. Phys. Lett.* **2003**, *371*, 189.